International Journal of Molecular and Clinical Microbiology 10(1) (2020) 1258-1274

International Journal of
Molecular and Clinical Microbiology

Effects of *Citrus limon (L.)* essential oil on *Pseudomonas aeruginosa*: complemented with a computational approach; focus on quorum sensing

Arghavan Arjmandi, Khosrow Chehri*, Isaac Karimi

Department of Biology, Faculty of Science, Razi University, Kermanshah, Iran

ARTICLE INFO

Article history:
Received 3 April 2020
Accepted 18 May 2020
Available online 1 June 2020

Keywords:
Pseudomonas aeruginosa,
Citrus limon,
molecular docking,
biofilm,
essential oil

ABSTRACT

Antibiotic-resistance is becoming an increasingly important concern. Resistant bacteria like *Pseudomonas aeruginosa* have different strategies while encountering either the immune system or antibiotics. As an example biofilm formation or quorum sensing can be mentioned as bacterial mechanisms to gain resistance. Therefore, it is crucial to explore novel compounds that might disrupt biofilm production especially using organic and plant-based compounds. *Citrus limon* essential oil has been used against multiple types of microorganisms in traditional medicine. The purpose of this study is to investigate the effect of this essential oil on *P. aeruginosa* biofilm formation. The inhibition of biofilm was measured using a micro-dilution method, staining the biofilm that has been formed and determining the minimum inhibitory concentration that proved effective. Then, via molecular docking software, the ligands more likely to interact with biofilm proteins were predicted. Our results suggest that after multiple determinations of minimum inhibitory concentration, the lowest effective dose was in concentrations between 100 µg/ml to around 450 µg/ml. Furthermore, molecular docking results demonstrated that between all the essential oil ligands, the top three were geranyl acetate, α-terpineol, and β-bisabolene. To sum up, *Citrus limon* essential oil showed promising anti-quorum sensing properties and it can be considered as a source of antimicrobial formulation.

1. Introduction

Pseudomonas aeruginosa is the fourth most accountable microorganism involved in nosocomial infections (Akbari et al., 2015; Krämer et al., 2016). The *P. aeruginosa* has a very large DNA susceptible to mutation and antigen shifting which altered this bacterium as a highly resistant pathogen with an annual decrement in its response to antibiotics (Carroll et al., 2016). Cystic fibrosis and immunocompromised patients are extremely susceptible to this infection with the danger of death being present when this pathogen attacks their immune system (Govan et al., 1996). On the other hand, this bacterium is gaining resistance to different types of antibiotics as the years go by (Poole et al., 1993; Rossolini et al., 2014). Indicating that soon all known antibiotics will fail to work on this pathogen. Consequently, finding new antimicrobial agents that are effective against this bacterium can be lifesaving in the case of many immunocompromised individuals.

As it was mentioned before, antigen shifting plays a major role in the resistance of this bacterium against antibiotics (Carroll et al., 2016). Apart from antigen shifting, the bacteria

*Corresponding author: Dr. Khosrow Chehri
E-mail address: khchehri@gmail.com

have another survival mechanism that protects them from the immune system, dubbed quorum sensing. This mechanism triggers the formation of biofilm, a very dense and adhesive structure, that acts as a physical barrier and protecting the bacteria from both antibodies and antibiotics. As a result, targeting this mechanism in antibiotic drug development stages is considered an effective way of controlling this bacterium. Following the attachment of the bacteria to a surface inside the body, the synthesis of an extracellular polysaccharide named N-Acyl homoserine lactone (AHL) is initiated which acts as a signaling molecule. After the cells reach a certain density, quorum sensing is triggered and other *P. aeruginosa* cells have received enough of the aforementioned signaling molecule to assure the existence of a sufficient population. As a result, other metabolites and proteins are released to help create the biofilm by activating the expression of critical genes. In *P. aeruginosa*, quorum sensing has two interacted pathways, LasR-LasI and RhlR-RhlI (Fuqua et al., 1994). The main enzyme responsible for the LasR-LasI pathway is transcriptional regulator LasR, which works alongside an acyl-homoserine-lactone synthase named LasI. When the density of AHL reaches to a certain point, regulatory protein RhlR genes are activated and as a result of this enzyme being present in the cell, another acyl-homoserine-lactone synthase known as RhlI is activated and signals the start of a series of cascade reactions; switching on all the other biofilm formation genes (Fuqua et al., 1994). The main proteins and their properties are as follows: Vfr (2OZ6) which regulates *P. aeruginosa* virulence, functions as a catabolite repressor inducing lasR transcription. RelA is a protein that is not present in the protein data bank so it was modeled using the SWISSMODEL website (*vide infra*). The template proteins on average respectively, had the sequence identity, sequence similarity, and coverage of 46.66, 0.43, and 0.98. It is modeled after different GTP pyrophosphokinases in other biofilm-forming bacteria which in the case of amino acid starvation. RelA induces lasR and rhlR expression and boosts acyl-HSL production. The template proteins for GacA on average had the sequence identity, sequence similarity, and coverage of 33.81, 0.38, and 0.98. They were modeled after VraR proteins. GacA is thought to activate the gene expression of RsmZ and RsmA. The protein BswR (4O8B) turns on the gene expression of RsmZ. ANR/FNR proteins are modeled after FNR type regulator in other bacteria with the sequence identity, sequence similarity, and coverage of 52.6, 0.45, and 0.94. These proteins activate during anaerobic conditions. The main quorum sensing factor is LasRI (4NG2) which activates or inhibits the second quorum sensing system by controlling RhlRI. (Schuster and Peter Greenberg, 2006).

Citrus limon (L.), from the *Rutaceae* family, offers many beneficial secondary metabolites (Zhang et al., 2015). The main substances found in *Citrus limon* extracts are alkaloids, flavonoids, coumarins, and phenols. The *Citrus limon* essential oil (CLEO) that is derived from its fruit peel has a specific "citrus" scent, which is because of "limonene"; this monoterpene alongside α-pinene are the two main components of CLEO (Lota et al., 2002) with antioxidative and antibacterial properties (Velu et al., 2014). In the last three decades, numerous papers have been published regarding the antibacterial activity of CLEO (Kerekes et al., 2013; Guzeldag et al., 2014; Ozogul et al., 2015). This study was aimed to investigate *in vitro* anti-pseudomonal effects of a CLEO and its fractions and to propose hypothetical mechanisms behind it using *in silico* tools. Targeting biofilm formation proteins is a novel method regarding the effects of CLEO on the formation of this structure, other studies tended to focus on solely the vital proteins. Therefore, a study that evaluates the ability of this formulation in biofilm inhibition seems necessary. The CLEO has many ligands that might bond to main biofilm proteins and alter their functionality. We were able to pinpoint exactly what these shifts in functionality are and what ligand causes them by individually checking the data in molecular docking software and then performing complementary tests on different organic solvent fractions. Additionally, this leads to highlighting the pathway that these changes might occur.

2. Methods and Materials

2.1. Preparing the essential oil (EO) fractions

Fresh lemons were purchased from Fasa, Shiraz, Iran. The first step was to grate the lemon peel, and after adding water the suspension was poured into a "Clevenger

apparatus" which is a steam distillation device purchased from Pyrexfan company, based in Iran. After about two hours, 5 ml of CLEO could be apprehended as an organic phase on top of the distilled water. Both phases were retrieved in one vial using the already installed valve on the Clevenger apparatus. The suspension was poured equally into four vials for acquiring fractions of CLEO. Three of these vials were made into different solvent fractions by adding diethyl ether, hexane, or xylene and extracting the organic phase. All solvents were purchased from Merck, which is based in Germany. After the evaporation of these solvents, the fractions were ready to use (Ferhat et al., 2007).

2.2. Serial dilutions

After the calculation of each CLEO density, a serial micro-dilution was made in polycarbonate 96-well plates using acetone. The CLEO with 500 µg/mL concentration was added in the first well, and the containing liquid after the addition of Merck trypticase soy broth (TSB) media was pipetted to create a 2-fold serial dilution decreasing in concentration from 500 µg/mL to 31 µg/mL. Sigma-Aldrich Triton X100 was used in 0.02% concentration as a surfactant to homogenize the organic-aqueous phases of CLEO and TSB media. In the negative control wells (31 µg/mL) no bacteria were added. Conveying that only the broth media and CLEO were present. Typically, no bacterial growth is expected in the negative control wells, whereas in the positive control wells, which consists of TSB media and bacterial suspension with no added CLEO, maximum bacterial growth is usually expected. For each fraction, three identical serial dilutions were made. After the serial dilution was ready, 10 µL of bacterial suspension of *Pseudomonas aeruginosa* ATCC27853 (0.5 McFarland standard) was added to all wells except negative control wells. The bacteria were purchased from Abosina company, Iran. As for the positive control wells, single bacterial suspension and TSB media were added. It is worth mentioning that Triton X100 does not have any effect on *P. aeruginosa* in the concentration used in our study (Yang et al., 2017). After the acetone was evaporated completely, the plate was wrapped tightly via sterile Clingfilm to prevent the evaporation of the CLEO, and then it was incubated. After incubation at 37°c for 18-24 hours was finished, the bacteria had developed both planktonic cell growth and biofilm formation. These biofilms are visible to the naked eye when the plate is moved, because you can observe that they move slightly but are also attached to the wells, but they are not distinguishable from planktonic cell growth in the photos. As a result, the biofilm has to be stained, but before that the planktonic cell growth has to be washed off (Wiegand et al., 2008).

2.3. Staining the biofilm and minimum inhibitory concentration (MIC) evaluation

First, the wells were washed with Sigma-Aldrich phosphate-buffered saline solution (PBS) to discard the excess media and the planktonic cell growth. Next, a solution of 20% crystal violet was added to each well to stain the biofilm for 20 minutes. Then, any excess crystal violet was washed off with PBS and ethanol carefully. Although the biofilm is mostly attached to the walls of the well, this step had to be done with extreme caution because this adhesion was very delicate. Lastly, the 96-well plate was put in the American Biotek ELx800 ELISA reader device at 630 nm for a second time to measure the influence of CLEO inclusion on biofilm formation. This is known as the Crystal violet biofilm staining method, introduced by O'Toole et al. (O'Toole et al., 2011). The optical densities were entered in a chart and the MIC was calculated by GraphPad Prism software function for MIC estimation. This function uses the optical density of the negative control well, and by creating a graph from the optical densities and different concentrations used in the experiment, calculates the minimum concentration that has inhibited bacterial cell growth (Figures 2 to 5). The approximate minimum inhibitory concentration can also be observed by the naked eye as the well that has no bacterial growth inside, which is the first clear-looking well.

2.4. Computer modeling and molecular docking

After determining the phytocompounds present in the CLEO, they were searched through the PubChem database (pubchem.ncbi.nlm.nih.gov). Their structure files were downloaded to be used in the docking

process. The ligand structures and their chemical properties are shown in Tables 1 and 2.

The next step was searching for the proteomics of *P. aeruginosa* and outlining the proteins responsible for biofilm formation and quorum sensing (Schuster and Peter Greenberg, 2006). To retain the protein structures the primary database approached was PDB (rcsb.org). In the case of the proteins in which their structure could not be traced online, the gene sequences were found in NCBI (ncbi.nlm.nih.gov), and their FASTA which is the code for amino acids available in proteins was then used in SWISSMODEL (swissmodel.expasy.org) to create their 3D models, with sequence identities ranging between 46 and 52.

These structure files were apprehended and alongside the ligand structure files using Molegro Virtual Docker and Chimera 1.8.1, got trimmed, hydrogenated, their energy minimized, dock-prepped, and checked for possible structure errors before adding them in PyRx, which is a software in molecular docking. The AutoDocking VINA wizard function was used in this study to calculate the binding affinities between the key proteins in biofilm formation and selected phytocompounds found in CLEO (Figure 1). By measuring the binding affinity, we can get a sense of how much a particular ligand might get close to a protein; the more negative the number of binding affinities are, the more likely it is for the protein and ligand to dock.

The docking space was intentionally limited to each protein's active sites. Eventually, since the number given as the affinity, is not solely enough in concluding whether or not the molecules are docked, another program known as LigPlot^{+} was used. This software demonstrates and depicts closely how two molecules can be docked together, and it shows the number and position of hydrophobic and hydrogen bonds.

2.5. Statistical analysis

A mathematical function can be calculated exclusive to each set of data and it can be used to compute the inhibitory concentration fifty (IC_{50}), which are both also shown in Table 3. The IC_{50} is the concentration in which 50% of all microorganisms were inhibited. The mean and standard deviation (SD) and standard error of the mean (SEM) are also reported in Table 3.

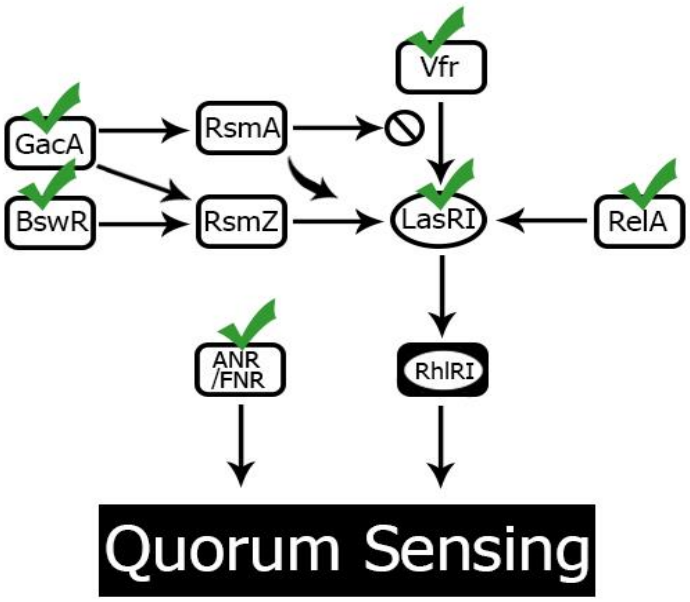

Figure 1. Proteins responsible for activating quorum sensing in Pseudomonas Aeruginosa. The protein boxes striked with a check mark were the ones targeted by CLEO ligands in this study. RsmZ and RhlR were not targeted since their gene sequences have not been presented yet. RsmA not only cannot activate quorum sensing without RsmZ, but in the absence of RsmZ, represses the synthesis of acyl-HSL which has a key role in quorum sensing (Greenberg et al., 2006)

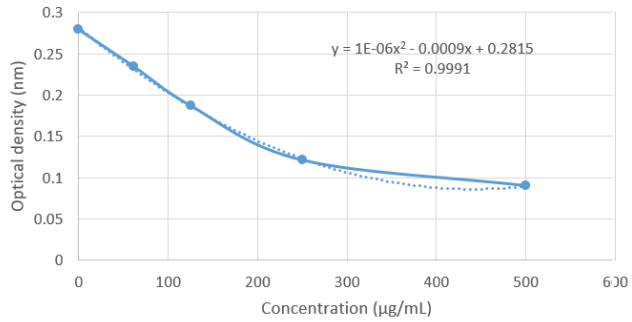

Figure 2. Essential oil trendline and function

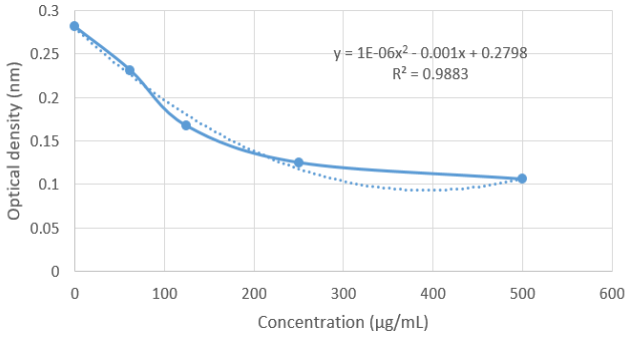

Figure 4. Hexane fraction trendline and function

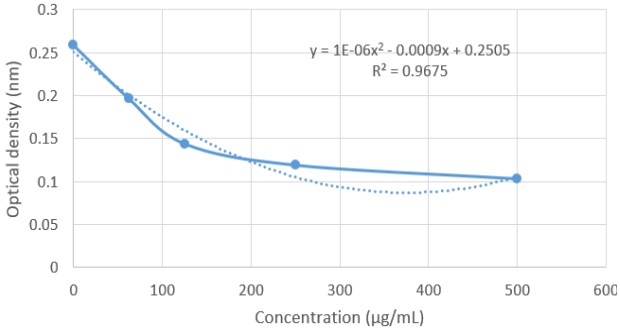

Figure 3. Diethyl ether fraction trendline and function

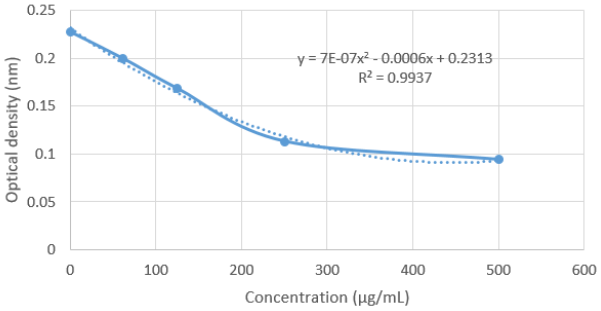

Figure 5. Xylene fraction trendline and function

Table 1. The properties of proteins responsible in activation and boosting of quorum sensing in *Pseudomonas Aeruginosa*.

Protein	**PDB**	**SWISS-MODEL**			**Target Protein properties**
		Average Sequence identity	**Average Sequence similarity**	**Average Coverage**	
Vfr	2OZ6	-	-	-	Regulates P. aeruginosa virulence functions as a catabolite repressor, induces lasR transcription
RelA	-	46.66	0.43	0.98	Model: GTP pyrophosphokinase, in case of amino acid starvation, induces lasR and rhlR expression and boosts acyl-HSL production
GacA	-	33.81	0.38	0.98	Model: VraR, Activates the gene expression of RsmZ and RsmA
BswR	4O8B	-	-	-	Activates the gene expression of RsmZ.
RsmZ	-	-	-	-	With the help of RsmA, activates LasR. Without it the expression of LasR is blocked.
ANR/FNR	-	52.61	0.45	0.94	Model: FNR type regulator, activates during anaerobic conditions.
LasRI	4NG2	-	-	-	Main quorum sensing factor.
RhlRI	-	-	-	-	Second quorum sensing system.

van Delden et al., 2001([6])

Table 2. CLEO compounds and their structures

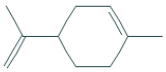	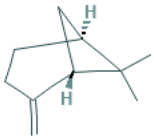	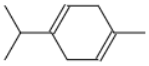	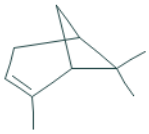
imonene	Beta-Pinene	Gamma-Terpinene	Alpha-Pinene
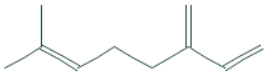	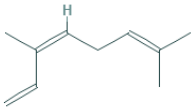	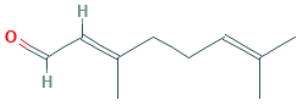	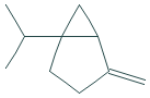
Myrcene	cis-Beta-Ocimene	Geranial (Citral)	Sabinene
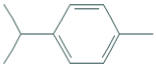	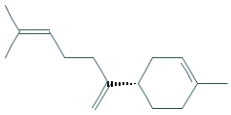	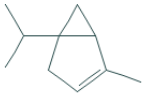	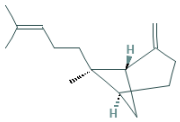
P-Cymene	Beta-Bisabolene	Alpha-thujene	trans-Beta-Bergamotene
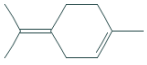	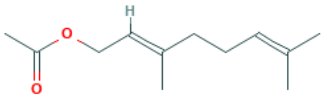	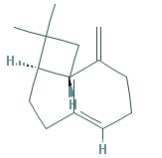	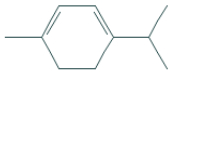
Terpinolene	Geranyl Acetate	Beta-Caryophyllene	Alpha-Terpinene
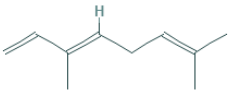	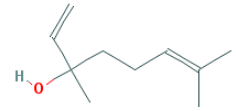	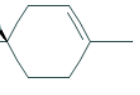	
trans-Beta-Ocimene	Linalool	Alpha-Terpineol	

pubchem.ncbi.nlm.nih.gov [17]

Table 3. CLEO compounds and their chemical properties

Phytochemical	PubChem CID	xlogP	Topological Polar Surface Area (A^2)	H-bond donors	H-bond acceptors	Molecular weight(g/mol)
Limonene	22311	3.4	0	0	0	136.238
Beta-Pinene	440967	3.1	0	0	0	136.238
Gamma-Terpinene	7461	2.8	0	0	0	136.238
Alpha-Pinene	6654	2.8	0	0	0	136.238
Myrcene	31253	4.3	0	0	0	136.238
cis-Beta-Ocimene	5320250	4.3	0	0	0	136.238
Geranial (Citral)	638011	3	17.1	1	0	152.237
Sabinene	18818	3.1	0	0	0	136.238
P-Cymene	7463	4.1	0	0	0	134.222
Beta-Bisabolene	10104370	5.2	0	0	0	204.357
Alpha-thujene	17868	2.8	0	0	0	136.238
trans-Beta-Bergamotene	12300069	5.1	0	0	0	204.357
Terpinolene	11463	2.8	0	0	0	136.238
Geranyl Acetate	1549026	3.5	26.3	0	2	196.29
Beta-Caryophyllene	5281515	4.4	0	0	0	204.357
Alpha-Terpinene	7462	2.8	0	0	0	136.238
trans-Beta-Ocimene	5281553	4.3	0	0	0	136.238
Linalool	6549	2.7	20.2	1	1	154.253
Alpha-Terpineol	443162	1.8	20.2	1	1	154.253

zinc.docking.org [18]

3. Results

3.1 In vitro

Each fraction elicited a different MIC. By representing the concentration and optical density (OD) data on a graph, a more accurate concentration amount for MIC can be calculated using Graphpad Prism software. It was demonstrated that the diethyl ether fraction presented the MIC of 232.2 µg/mL. Furthermore, the MIC of hexane and xylene fraction were 251.7 and 323.8 µg/mL, respectively, whereas the MIC of non-fractioned CLEO was 351.6 µg/mL. In Table 3 the calculated MIC values are reported.

Results from the diethyl ether fraction indicated an IC_{50} of 135.3 µg/mL, and respective IC_{50} of 140.0 µg/mL and 197.6 µg/mL for hexane and xylene fractions were calculated. The IC_{50} of non-fractioned CLEO was 158.6 µg/mL. Since all experiments were carried out three times, the average of a set of three MICs was calculated and used to depict a single graph and function. These graphs are shown in Figures 2 to 5.

After washing off the excess planktonic growth, the biofilm stayed intact in the wells since there has already been an adhesion to the surface for the biofilm to be formed. After using crystal violet suspension for staining the biofilm structure as mentioned before (Figure 6), the results indicated that although CLEO has antibacterial effects against planktonic growth in *P. aeruginosa*, the main antibacterial effects of this EO is through controlling the biofilm formation in this bacterium. By adding acetic acid to the wells, all crystal violet stains will be solved in the acid and so it will have been made easier to see and compare the intensity of the color in each well (Figure 7).

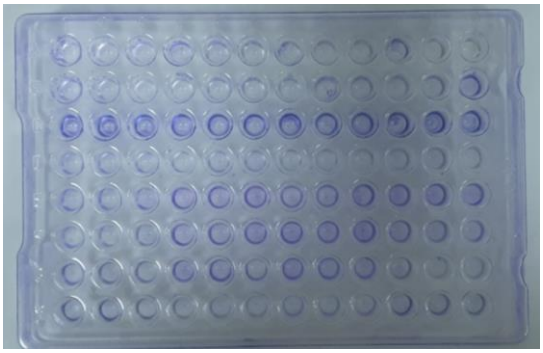

Figure 6. Biofilm stained with crystal violet can be seen as darker violet masses, near the edges

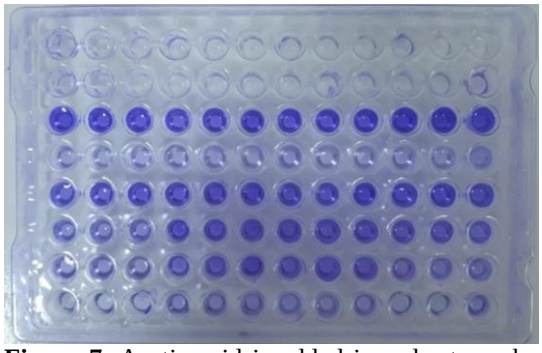

Figure 7. Acetic acid is added in order to make the color differentiation obvious to the naked eye

3.2. In silico

In Table 4, all the affinities between -6.0 to -10.0 were conventionally shown. It is worth mentioning that among GacA, RelA, and BswR, none of the binding affinities were lesser than -6.0, therefore the best docked ligand-protein pairs were summarized in Table 4.

The geranyl acetate–Vfr scene with four hydrogen bonds demonstrated the highest number of this significant type of intermolecular interactions. The highest number of hydrophobic bonds, which was 29, belonged to this protein-ligand combination as well. Ligand-protein scenes displaying the best binding affinities and hydrophobic bond numbers can be seen in Table 5. The scenes and the bonds of the top results in docking are depicted in Figures 8 to 23.

The scenes with the best binding affinities were β-Bisabolene – LasR, *trans*-α-Bergamotene – LasR and β-Caryophyllene – LasR, and the highest number of hydrophobic bonds belonged to Geranyl acetate – Vfr, Limonene – LasR, β-Bisabolene – LasR and β-Pinene – Vfr. The Geranyl acetate – Vfr scene with four hydrogen bonds appeared to be the most active scene in this matter. Followed by the α-Terpineol – LasR scene and the α-Terpineol – FNR scene respectively presenting two and one possible hydrogen bonds.

This scene presents 29 possible hydrophobic bonds (Table 5) and 4 possible hydrogen bonds (Figure 8). Three of these bonds potentially were between the acetate group of this molecule and Ser76, with the shortest bond (2.78 Å) being between the G oxygen in the amino acid and the oxygen number one of the acetate group, belonging to the ligand. The bond between the oxygen number two of the ligand and the G oxygen in Ser76 was the second shortest with it being 2.92 Å. The next bond regarding its length (2.94 Å) was between the same oxygen of the ligand but with Ala77 from the protein. The longest bond, 3.06 Å, was between the nitrogen group of Ser76 and the oxygen number two of the ligand. All the hydrogen bonds appear to belong to the acetate group of geranyl acetate.

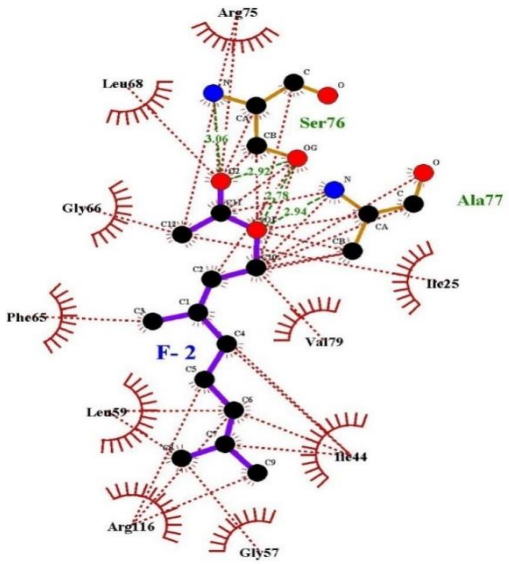

Figure 8. The two dimensional illustration of Geranyl acetate and vfr interactions in LigPlot+

The α-Terpineol and LasR scene (Figure 9) predicts the only oxygen in α-Terpineol formed two hydrogen bonds with the shortest one being 2.71 Å to the D2 oxygen of Asp72, and the long bond (2.92 Å) was calculated to form with the OH group of Tyr63. The last hydrogen bond was in the scene of α-Terpineol and FNR which is shown in Figure 10. In this scene, again, the only oxygen in α-Terpineol seems to have established a 2.78 Å bond with the E2 oxygen of Glu99.

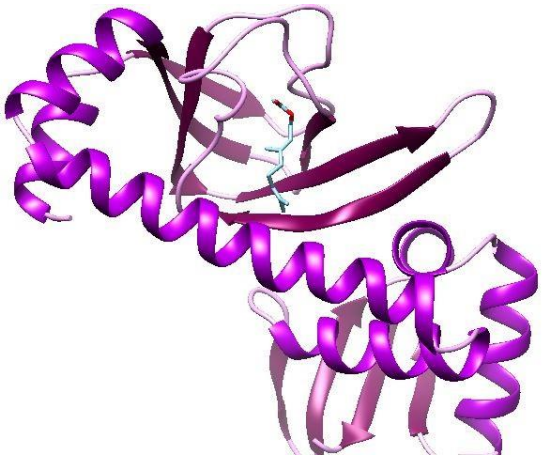

Figure 9. Geranyl acetate and vfr scene in 3D, captured via Chimera

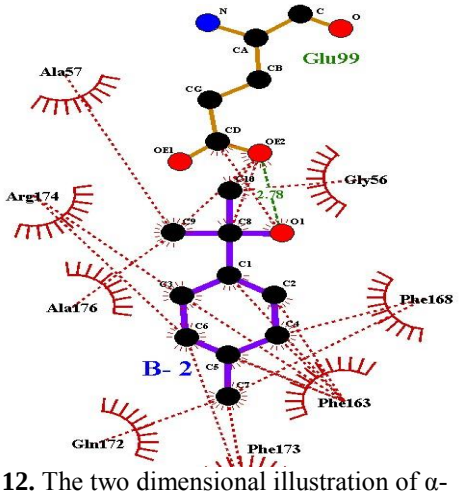

Figure 12. The two dimensional illustration of α-Terpineol and FNR interactions in LigPlot+

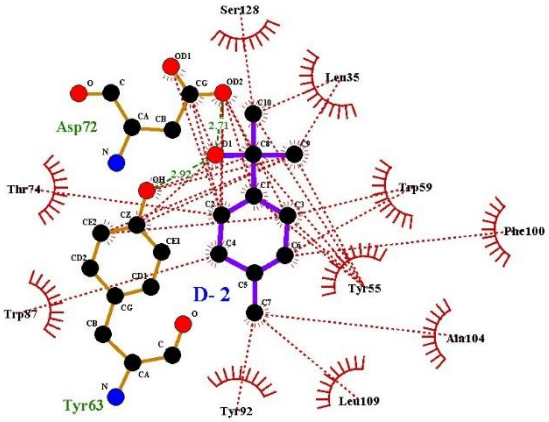

Figure 10. The two dimensional illustration of α-Terpineol and LasR interactions in LigPlot+

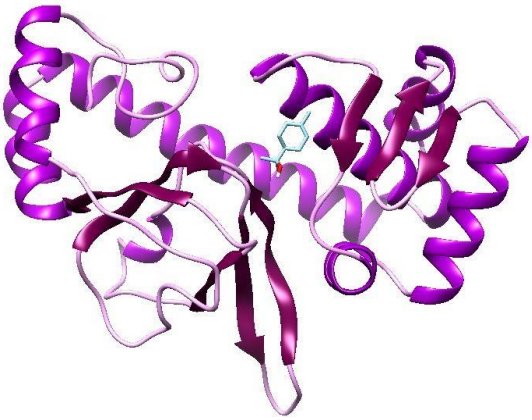

Figure 13. α-Terpineol and FNR scene in 3D, captured via Chimera

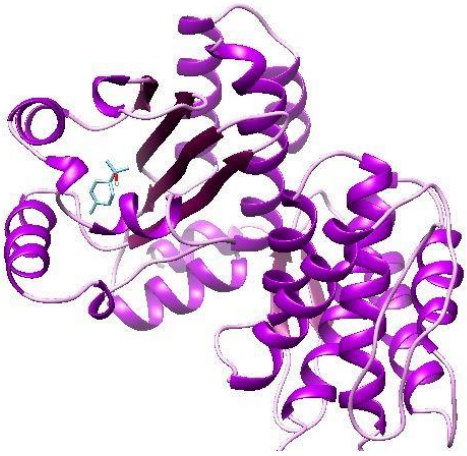

Figure 11. α-Terpineol and LasR scene in 3D, captured via Chimera

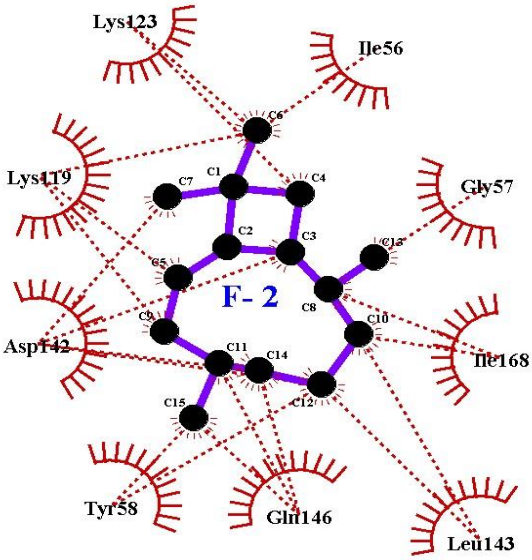

Figure 14. The two dimensional illustration of β-Caryophyllene and Vfr interactions in LigPlot+

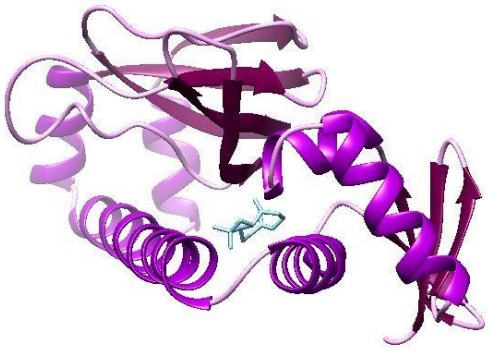

Figure 15. β-Caryophyllene and Vfr scene in 3D, captured via Chimera

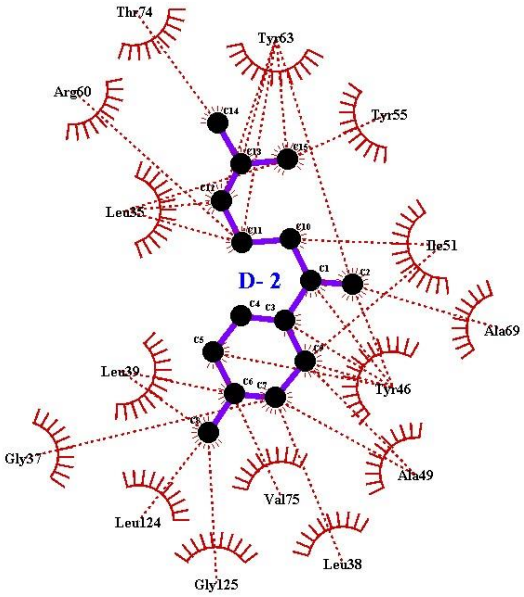

Figure 16. The two dimensional illustration of β-Bisabolene and LasR interactions in LigPlot+

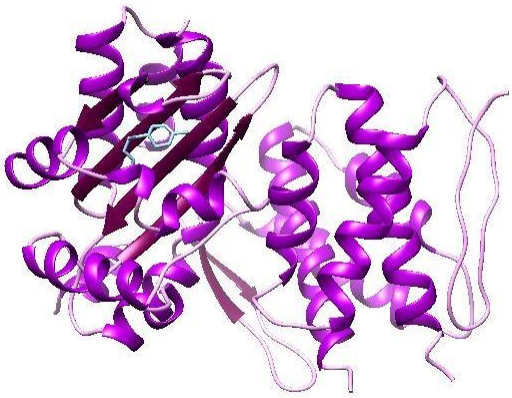

Figure 17. β-Bisabolene and LasR scene in 3D, captured via Chimera

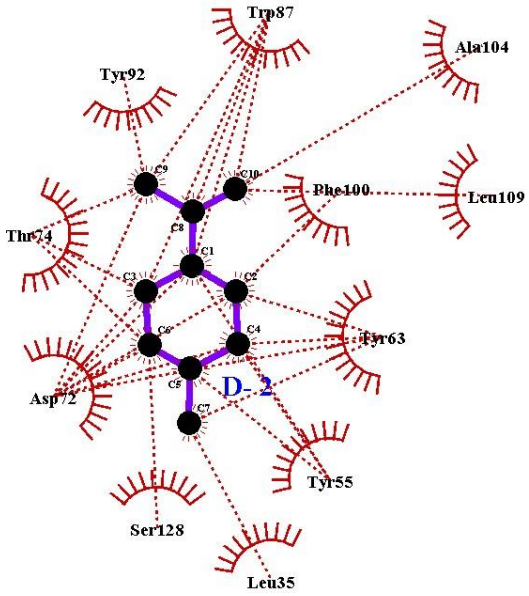

Figure 18. The two dimensional illustration of Limonene and LasR interactions in LigPlot+

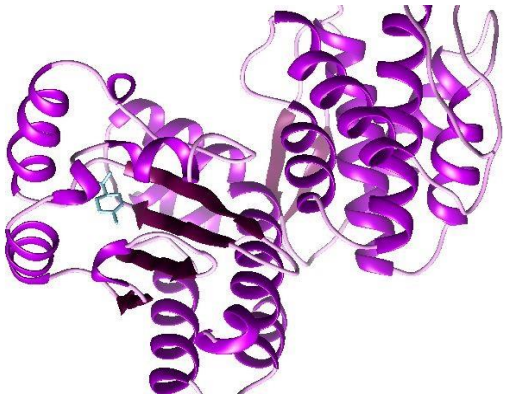

Figure 19. Limonene and LasR scene in 3D, captured via Chimera

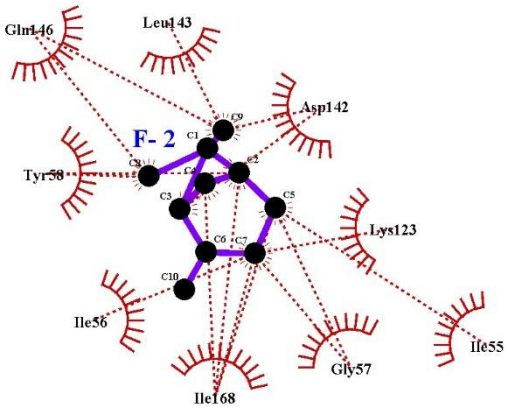

Figure 20. The two dimensional illustration of β-Pinene and Vfr interactions in LigPlot+

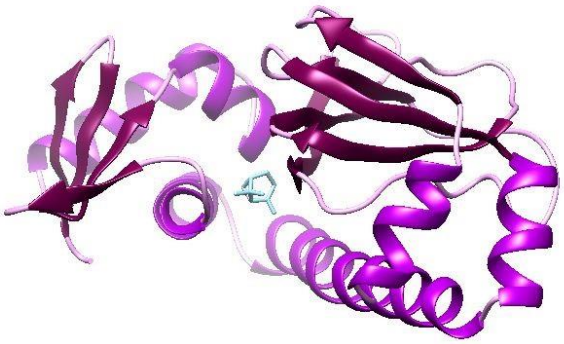

Figure 21. β-Pinene and Vfr scene in 3D, captured via Chimera

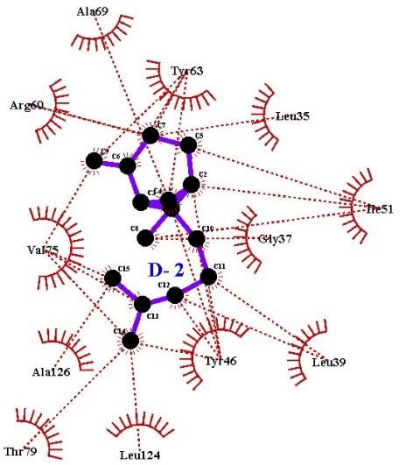

Figure 22. The two dimensional illustration of trans-α-Bergamotene and LasR interactions in LigPlot+

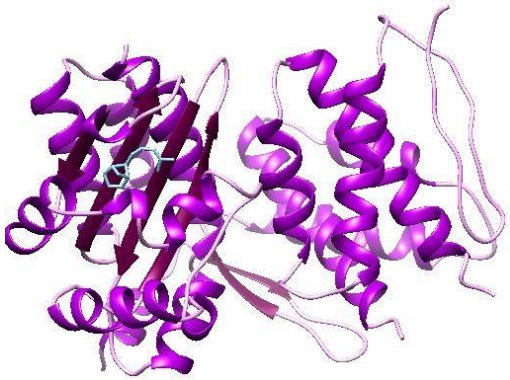

Figure 23. trans-α-Bergamotene and LasR scene in 3D, captured via Chimera

Table 4. MIC after washing off the planktonic cells and staining the biofilm with crystal violet. The IC50 value is calculated based on the graph function of individual averages of datasets. All tests were carried out three times.

Type	MIC µg/mL	Function	R^2	IC50 µg/mL	SD	SEM
Essential oil	351.6	$y = 1E\text{-}06x^2 – 0.0009x + 0.2815$	0.999	158.6	18.1	10.4
Diethyl ether fraction	232.2	$y = 1E\text{-}06x^2 – 0.0009x + 0.2505$	0.967	135.3	28.1	16.2
Hexane fraction	251.7	$y = 1E\text{-}06x^2 – 0.001x + 0.2798$	0.988	140.0	14.7	8.5
Xylene fraction	323.8	$y = 7E\text{-}07x^2 – 0.0006x + 0.2313$	0.993	197.6	19.4	11.2

Table 5. Highest binding affinities and highest hydrophobic bond numbers

Protein - Ligand	Binding affinity	Hydrophobic bond numbers
BswR - trans-α-Bergamotene	-5.4	14
FNR - *β* -Bisabolene	-6.3	**23**
FNR - trans-α-Bergamotene	-6.2	**21**
FNR - *β*-Caryophyllene	-6.5	**22**
FNR - α-Terpineol	-6.1	17
GacA - γ-Terpinene	-5.1	14
LasR - Limonene	-6.7	**27**
LasR - *β*-Pinene	-6.5	15
LasR - γ-Terpinene	-7.0	19
LasR - α-Pinene	-6.5	14
LasR - cis-*β*-Ocimene	-6.1	19
LasR - Geranial	-6.0	**21**
LasR - Sabinene	-6.3	14
LasR - ρ-Cymene	-7.0	**23**
LasR - *β*-Bisabolene	-8.4	**26**
LasR - α-Thujene	-6.4	15
LasR - trans-α-Bergamotene	-7.8	**22**
LasR - Terpinolene	-6.9	14
LasR - α-Terpinene	-0.7	**22**
LasR - trans-*β*-Ocimene	-6.1	17
LasR - α-Terpineol	-6.6	**21**
RelA - trans-α-Bergamotene	-6.2	16
Vfr - *β*-Pinene	-6.0	**26**
Vfr - *β*-Bisabolene	-6.8	**24**
Vfr - trans-α-Bergamotene	-6.5	**24**
Vfr - Geranyl acetate	-6.4	**29**
Vfr - *β*-Caryophyllene	-7.3	19
Vfr - α-Terpineol	-6.0	**22**

Table 6. best docking results in binding affinity, number of hydrophobic bonds and Hydrogen bonds

Top binding affinities	**Highest number of Hydrophobic bonds**	**Hydrogen bonds between ligand and proteins**
β-Bisabolene – LasR: -8.4	Geranyl acetate – Vfr: 29	Geranyl acetate – Vfr: Four hydrogen bonds
trans-α-Bergamotene – LasR: -7.8	Limonene – LasR: 27	α-Terpineol – LasR: Two hydrogen bonds
β-Caryophyllene – Vfr: -7.3	β-Bisabolene – LasR: 26	α-Terpineol – FNR: one hydrogen bond
	β-Pinene – Vfr: 26	

Table 7. an estimation on which ligands are more present in each fraction, and which ligands are less soluble in them based on molecular polar surface area and XlogP (a negative sign means less solubility and a positive sign means more solubility).

	EO	Diethyl ether fraction	Xylene fraction	Hexane fraction
Compounds present	All	All + geranial, + geranyl acetate + α-terpineol	All - α-terpineol	All - α-terpineol + β-Caryophyllene + β-Bisabolene, + trans-α-Bergamotene

4. Discussion

For millions of years, plants have been protecting themselves and their fruit that contains seeds, from bacteria in a never-ending evolutionary war. Therefore, using plant material which is also easily accessible appears as an acceptable choice for new antimicrobial agents. These compounds also must be soluble in lipids. This is measured by the octanol/water partition coefficient (LogP), which has to be above 1 (Cheng et al., 2007). Consequently, using EOs is more reasonable in this sense than using extracts, since the EO has a higher LogP than the latter because extracts are hydrophilic. It should be mentioned that the MICs and IC_{50}s reported in our study are acceptable but not majorly ideal for consideration of CLEO as a whole against the bacteria. As a result, individual ligands from this EO have to be investigated in depth. The focus of this study was on the fact that certain fractions appear to have reduced the biofilm production more, implying that the ligands that were more plentiful in these fractions might be active against biofilm formation. The higher the polar surface area number of a ligand, the more it can be solved in a diethyl-ether fraction in general. The fact that using diethyl-ether decreased the MIC, and the molecule with the highest number for polar surface area happened to be the best result of our *in silico* studies, suggests that in theory this chemical, geranyl acetate, might be able to give better results when used individually. These ligands were very close to being in the top docking results but they were bested by some other compounds like β-Caryophyllene, β-Bisabolene, and *trans*-α-Bergamotene. These ligands have relatively high LogP. Our theory is that as a result, they will probably be more soluble in solvents that are more hydrophobic, meaning that the more hydrophobic a solvent is, the more we expect to see these ligands in it. Since it was established in our *in silico* studies that these compounds might have effects on the biofilm formation, the hexane fraction with the logP of 3.9 by showing a lower MIC than the Xylene fraction with the logP of 3.2, indicated that they have an inhibitory effect against the biofilm formation process. The *in silico* studies suggest this is achieved by interacting with three key proteins responsible for Quorum sensing; LasR, FNR, and Vfr.

The diethyl ether fraction produced the best results, meaning that it had the lowest MIC and IC_{50} values, proving to be the most practical CLEO fraction against biofilm formation in *P. aeruginosa*. After that fraction, hexane and xylene fractions were respectively more powerful in controlling the biofilm, comparing to the CLEO. In the "*in silico"* studies, between our top results, geranyl acetate proved to be the most docked ligand to biofilm formation key proteins. This ligand has a low XlogP value and a high polar surface area and therefore it was estimated to be more present in the diethyl ether fraction than in other fractions. The diethyl ether

fraction has more geranial, geranyl acetate, and α-terpineol present because these molecules have polar surface areas and this solvent is attracted to these types of compounds. The xylene fraction has less α-terpineol because this compound has a very low XlogP (1.8) and is slightly less soluble in a solvent with high XlogP, like xylene or hexane. On the other hand, hexane has a higher XlogP than xylene, and as a result, it can be concluded that ligands with high XlogP like β-Caryophyllene, β-Bisabolene, and *trans*-α-Bergamotene will be more abundant in this fraction. These findings were based on the XlogP and polar surface area of each solvent and ligand. Hexane proved to be the most powerful solvent for hydrophobic molecules in this study and therefore the number of hydrophobic ligands was predicted to be slightly higher in this fraction and xylene, which also has a high XlogP. These ligands are β-Caryophyllene, β-Bisabolene, and trans-α-Bergamotene. Hexane has a higher XlogP value than Xylene, which explains why it showed a better MIC value comparing to the Xylene fraction and CLEO. Finally, it can be stated that geranyl acetate, α-Terpineol, β-bisabolene, trans-α-bergamotene, β-caryophyllene, limonene, and β-pinene have the potential to inhibit biofilm formation by interacting with Vfr, FNR, and LasR respectively which are all vital proteins in the quorum sensing of *Pseudomonas aeruginosa*.

Limonene is the most abundant ligand in CLEO, The IUPAC name for limonene is 1-Methyl-4-(prop-1-en-2-yl) cyclohex-1-ene (pubchem.ncbi.nlm.nih.gov). *E. coli* O157:H7, *Salmonella* species, and *Bacillus pusillus* appear to be susceptible to limonene (Nannapaneni et al., 2008; O'Bryan et al., 2008; Sonboli et al., 2011). Although it is relatively effective against bacteria in a study about its antifungal abilities, it was stated that this molecule is not successful in controlling three *Aspergillus* species (Kim and Park, 2012). *Mycoplasma pneumonia* is a lot more susceptible to limonene comparing to bergamot EO, suggesting that limonene is very active in bergamot EO (Furneri et al., 2012). This further proves our findings, that limonene one of the most active chemical agents present in *Citrus* species. Limonene extracted from *Artemisia capillaris* was most effective against a clinical strain of *E. coli*, which is consistent with the Nannapaneni et al. study that was mentioned before (Yang et al., 2014). The fact that multiple studies are supporting the theory that limonene is active against gram-negative biofilm-producing bacteria like *E. Coli* (Nannapaneni et al.; Yang et al., 2014; Sakar et al., 2017) is in line with our findings on this compound being active against *Pseudomonas* since this is another biofilm-producing gram-negative bacteria. In the Sakar et al. study a binding affinity of -7.6 was reported for limonene against *E. coli* vital proteins (Sakar et al., 2017) whereas the best binding affinity for biofilm proteins of *P. aeruginosa* in our current study was -6.7 between limonene and LasR. Despite that, this scene was estimated by us to have 27 hydrophobic bonds meaning that this scene is among the top three regarding the number of hydrophobic bonds.

In our study, three ligands were assessed as the most active phytochemicals against biofilm formation in *P. aeruginosa* by both our *in silico* and *in vitro* studies. These compounds were geranyl acetate, α-Terpineol, and β-Bisabolene. Geranyl acetate was predicted to be the most active compound against *Pseudomonas* because it has four alleged hydrogen bonds with one of the main key proteins of biofilm formation which is Vfr. The IUPAC name for geranyl acetate is 3,7-Dimethyl-2,6-octadien-1-yl acetate (pubchem.ncbi.nlm.nih.gov). The Ser76 of this protein is hydrogen-bonded to both oxygens of geranyl acetate and the nitrogen atom of this amino acid is also hydrogen-bonded to the terminal oxygen atom of this ligand. In this protein, another hydrogen bond can be seen between oxygen #1 of the ligand with the terminal nitrogen atom of Ala77. Geranyl acetate also can have 29 hydrophobic bonds with Vfr according to our findings. Based on this study and the studies focused on this ligand, geranyl acetate seems to be an active agent against gram-negative bacteria. Consistent with our results indicating that geranyl acetate is a potent antimicrobial agent, it has lowered the MIC of *Candida* species (Zore et al., 2010), and it is considered effective against Mycobacterium tuberculosis, Escherichia coli ETEC 5041-1, Escherichia coli EPEC 0031-2, and the fungi *Candida albicans* (Vik et al., 2007; Duarte et al., 2007; Rajput and Karuppayil, 2013). This phytochemical was effective against *Saccharomyces cerevisiae* when used alongside geraniol (Prashar et al., 2003).

α-Terpineol is an isomer of an alcohol monoterpene named terpineol with the IUPAC name of 2-(4-Methylcyclohex-3-en-1-yl) propan-2-ol (pubchem.ncbi.nlm.nih.gov). In our study, this ligand successfully bonds to two key proteins in the biofilm formation of *P. aeruginosa*. These proteins are FNR and LasR. The latter can be named as the most important protein in quorum sensing (figure 1) because of its key role in the protein network. The terminal oxygen of α-Terpineol has hydrogen-bonded to the hydroxyl group of Tyr63 and the OD2 atom of Asp72. The same α-Terpineol terminal oxygen is hydrogen-bonded to OE2 of Glu99 in FNR. Although studies suggest that this ligand is more active against fungi like *Candida albicans* and *Cryptococcus neoformans* (Costa et al., 2000) and *Candida* species in general (Ramage et al., 2012), our research indicates that it might be active against some bacteria in the sense that it would block biofilm formation in them, but the researches done on biofilm formation are too limited at this moment and maybe a logical next step would be to investigate the anti-biofilm formation abilities in different bacterial species. This chemical was reported to be mutagenic to *Salmonella* species (Gomes-Carneiro et al., 1998).

β-Bisabolene ((*S*)-1-Methyl-4-(6-methylhepta-1,5-dien-2-yl) cyclohex-1-ene) is an isomer of a sesquiterpene known as bisabolene (pubchem.ncbi.nlm.nih.gov). Accordingly, β-bisabolene in the essential oil of *Bidens tripartita* root was reported to be highly active against fungi (Tomczykowa et al., 2011). In the current study, β-Bisabolene showed a great binding affinity with LasR while maintaining 26 hydrophobic bonds with this protein and 26 other hydrophobic bonds with Vfr. Suggesting that *P. aeruginosa* might be susceptible to this ligand. Despite that, there are surprisingly not enough studies to support the antibacterial properties of this phytochemical. One reason might be that the big size of this molecule prevents it from entering a lot of enzymatic active sites, and as a result, it can exclusively be active against proteins with major gaps in their active sites, like LasR.

In conclusion, CLEO can be considered a moderately active essential oil against *P. aeruginosa* biofilm formation, but as our data both in molecular modeling and the MICs from different EO fractions suggest there are some ligands present in this compound that are more active as anti-biofilm agents. Targeting biofilm formation in P. aeruginosa, and using different fractions to determine which ligand will be more effective against the biofilm, complemented with computational in silico studies is a novel approach, not taken by any other scientific researcher until now. The molecular docking results suggested that geranyl acetate, α-Terpineol, β-bisabolene, trans-α-bergamotene, β-caryophyllene, limonene, and β-pinene are ligands with the most antibacterial ability against P. aeruginosa. As a result, further investigation is necessary to determine with precision which ligand is more active and to what degree this antibacterial potential exists.

Acknowledgement

This paper originated from MSc thesis of Arghavan Arjmandi submitted to the Department of Biology, Faculty of Science, Razi University 67149-67346, Kermanshah, Iran. This study was supported by an intramural fund.

Conflicts of interest

There are no conflicts of interest.

Refereces

Sakar, E. A, Chehri, K., Karimi, N., & Karimi, I. (2017). Computational approaches to the in vitro antibacterial activity of Allium hirtifolium Boiss against gentamicin-resistant Escherichia coli: focus on ribosome recycling factor. In Silico Pharmacology, 5(1). doi: 10.1007/s40203-017-0027-z

Akbari, F. and Kjellerup, B. (2015). Elimination of Bloodstream Infections Associated with Candida albicans Biofilm in Intravascular Catheters. Pathogens, 4(3): 457-469.

Carroll, K. (2016). Jawetz, Melnick&Adelberg's medical microbiology. New York: McGraw-Hill Education.163- 307.

Cheng, T., Zhao, Y., Li, X., Lin, F., Xu, Y., Zhang, X., Li, Y., Wang, R. and Lai, L. (2007). Computation of Octanol−Water Partition Coefficients by Guiding an Additive Model with Knowledge. Journal of Chemical

Information and Modeling. 47(6): 2140-2148.

Costa, T., Fernandes, O., Santos, S., Oliveira, C., Lião, L., Ferri, P., Paula, J., Ferreira, H., Sales, B. and Silva, M. (2000). Antifungal activity of volatile constituents of Eugenia dysenterica leaf oil. Journal of Ethnopharmacology. 72(1-2): 111-117.

Duarte, M., Leme, E., Delarmelina, C., Soares, A., Figueira, G. and Sartoratto, A. (2007). Activity of essential oils from Brazilian medicinal plants on Escherichia coli. Journal of Ethnopharmacology. 111(2): 197-201.

Ferhat, M., Meklati, B. and Chemat, F. (2007). Comparison of different isolation methods of essential oil fromCitrus fruits: cold pressing, hydrodistillation and microwave 'dry' distillation. Flavour and Fragrance Journal. 22(6): 494-504.

Fuqua, W., Winans, S. and Greenberg, E. (1994). Quorum sensing in bacteria: theLuxR-LuxI family of cell density-responsive transcriptional regulators. Journal of Bacteriology. 176(2): 269-275.

Furneri, P., Mondello, L., Mandalari, G., Paolino, D., Dugo, P., Garozzo, A. and Bisignano, G. (2012). In vitro antimycoplasmal activity of citrus bergamia essential oil and its major components. European Journal of Medicinal Chemistry. 52: 66-69.

Gomes-Carneiro, M., Felzenszwalb, I. and Paumgartten, F. (1998). Mutagenicity testing of (±)-camphor, 1,8-cineole, citral, citronellal, (−)-menthol and terpineol with the Salmonella/microsome assay. Mutation Research/Genetic Toxicology and Environmental Mutagenesis. 416(1-2): 129-136

Govan, J. R. and Deretic, V. (1996). Microbial pathogenesis in cystic fibrosis: mucoid Pseudomonas aeruginosa and Burkholderia cepacia. Microbiological reviews. 60 (3): 539-574.

Guzeldag G., Kadioglu L., Mercimek A., Matyar F. (2014). Preliminary examination of herbal extracts on the inhibition of Helicobacter pylori. African Journal of Traditional Complementary Alternate Medicene. 11(1): 93-96

Kerekes, E., Deák, É., Takó, M., Tserennadmid, R., Petkovits, T., Vágvölgyi, C. and Krisch, J. (2013). Anti-biofilm forming and anti-quorum sensing activity of selected essential oils and their main components on food-related micro-organisms. Journal of Applied Microbiology, p.n/a-n/a.

Kim, E. and Park, I. (2012). Fumigant Antifungal Activity of Myrtaceae Essential Oils and Constituents from Leptospermum petersonii against Three Aspergillus Species. Molecules. 17(9): 10459-10469.

Krämer, A., Herzer, J., Overhage, J. and Meyer-Almes, F. (2016). Substrate specificity and function of acetylpolyamineamidohydrolases from Pseudomonas aeruginosa. BMC Biochemistry. 17(1) 120-128.

Lota, M., de Rocca Serra, D., Tomi, F., Jacquemond, C. and Casanova, J. (2002). Volatile Components of Peel and Leaf Oils of Lemon and Lime Species. Journal of Agricultural and Food Chemistry. 50(4): 796-805.

Nannapaneni, R., Muthaiyan, A., Crandall, P., Johnson, M., O'Bryan, C., Chalova, V., Callaway, T., Carroll, J., Arthington, J., Nisbet, D. and Ricke, S. (2008). Antimicrobial Activity of Commercial Citrus-Based Natural Extracts Against Escherichia coli O157:H7 Isolates and Mutant Strains. Foodborne Pathogens and Disease. 5(5): 695-699.

NCBI.nlm.nih.gov. (2018). National Center for Biotechnology Information. [online] Available at: https://www.ncbi.nlm.nih.gov/ [Accessed 5 Jan. 2018].

O'Bryan, C., Crandall, P., Chalova, V. and Ricke, S. (2008). Orange Essential Oils Antimicrobial Activities against Salmonella spp. Journal of Food Science. 73(6): M264-M267.

O'Toole, G. (2011). Microtiter Dish Biofilm Formation Assay. Journal Of Visualized Experiments, (47). doi: 10.3791/2437

Ozogul, Y., Kuley, E., Ucar, Y. and Ozogul, F. (2015). Antimicrobial Impacts of Essential Oils on Food Borne-

Pathogens. Recent Patents on Food, Nutrition & Agriculture. 7(1): 53-61.

Poole, K., Krebes, K., McNally, C., and Neshat, Sh. (1993). Multiple antibiotic resistance in Pseudomonas aeruginosa: evidence for involvement of an efflux operon. Journal of bacteriology. 175 (22): 7363-7372.

Prashar, A., Hili, P., Veness, R. and Evans, C. (2003). Antimicrobial action of palmarosa oil (Cymbopogonmartinii) on Saccharomyces cerevisiae. Phytochemistry. 63(5): 569-575.

Pubchem.ncbi.nlm.nih.gov. (2018). The PubChem Project. [online] Available at: https://pubchem.ncbi.nlm.nih.gov/ [Accessed 4 Sep. 2018].

Rajput, S. and Karuppayil, S. (2013). Small molecules inhibit growth, viability and ergosterol biosynthesis in Candida albicans. SpringerPlus. 2(1):26.

Ramage, G., Milligan, S., Lappin, D., Sherry, L., Sweeney, P., Williams, C., Bagg, J. and Culshaw, S. (2012). Antifungal, Cytotoxic, and Immunomodulatory Properties of Tea Tree Oil and Its Derivative Components: Potential Role in Management of Oral Candidosis in Cancer Patients. Frontiers in Microbiology. 3. 220.

Rossolini, G. M., Arena, F., Pecile, P., and Pollini, S. (2014). Update on the antibiotic resistance crisis. Current opinion in pharmacology. 18: 56-60

Schuster, M. and Peter Greenberg, E. (2006). A network of networks: Quorum-sensing gene regulation in Pseudomonas aeruginosa. International Journal of Medical Microbiology. 296(2-3): 73-81.

Sonboli, A., Gholipour, A. and Yousefzadi, M. (2012). Antibacterial activity of the essential oil and main components of two Dracocephalum species from Iran. Natural Product Research. 26(22): 2121-2125.

Swissmodel.expasy.org. (2018). SWISS-MODEL. [online] Available at: https://swissmodel.expasy.org.

Tomczykowa, M., Leszczyńska, K., Tomczyk, M., Tryniszewska, E. and Kalemba, D. (2011). Composition of the Essential Oil of Bidenstripartita L. Roots and Its Antibacterial and Antifungal Activities. Journal of Medicinal Food. 14(4): 428-433.

Velu, S., Abu bakar, F., Mahyudin, N., Saari, N. and Zaman, M. (2014). In vitro antimicrobial activity of musk lime, key lime and lemon extracts against food related pathogenic and spoilage bacteria. International Food Research Journal. 21(1): 379-386.

Vik, A., James, A. and Gundersen, L. (2007). Screening of Terpenes and Derivatives for Antimycobacterial Activity; Identification of Geranylgeraniol and Geranylgeranyl Acetate as Potent Inhibitors of Mycobacterium tuberculosis in vitro. Planta Medica. 73(13): 1410-1412.

Wiegand, I., Hilpert, K. and Hancock, R. (2008). Agar and broth dilution methods to determine the minimal inhibitory concentration (MIC) of antimicrobial substances. Nature Protocols. 3(2):163-175.

Yang, C., HU, D., & Feng, Y. (2014). Antibacterial activity and mode of action of the Artemisia capillaris essential oil and its constituents against respiratory tract infection-causing pathogens. Molecular Medicine Reports, 11(4), 2852-2860. doi: 10.3892/mmr.2014.3103

Yang, A., Tang, W. S., Si, T. and Tang, J.X. (2017). Influence of Physical Effects on the Swarming Motility of Pseudomonas aeruginosa. Biophysical Journal. 112:1462–1471.

Zinc.docking.org. (2018). Welcome to ZINC Is Not Commercial - A database of commercially-available compounds. [online] Available at: http://zinc.docking.org.

Zore, G., Thakre, A., Rathod, V. and Karuppayil, S. (2010). Evaluation of anti-Candida potential of geranium oil constituents against clinical isolates of Candida albicans differentially sensitive to fluconazole: inhibition of growth, dimorphism and sensitization. Mycoses. 54(4): e99-e109.